ELSEVIER

Journal of Alloys and Compounds 330–332 (2002) 262–267

Journal of ALLOYS AND COMPOUNDS

www.elsevier.com/locate/jallcom

# Study of the corrosion resistance of Cr, Zr, Y doped $AB_5$ type alloys in KOH

O. Arnaud[a,*], P. Barbic[b], P. Bernard[a], A. Bouvier[b], B. Knosp[a], B. Riegel[c], M. Wohlfahrt-Mehrens[c]

[a]*SAFT, Direction de la Recherche, 111 Bd. Alfred Daney, F-33074 Bordeaux Cedex, France*
[b]*Treibacher Auermet, Auer von Welsbachstrasse 1, A-9330 Treibach-Althofen, Austria*
[c]*ZSW, Helmholtzstrasse 8, D-89081 Ulm, Germany*

## Abstract

The effect of partial substitutions of Y, Zr or Cr on the chemical stability of $AB_{5+x}$ alloys in concentrated KOH aqueous solution was investigated. Alloys were elaborated using conventional casting, rapid cooling or gas atomisation, then heat-treated and characterised in terms of chemical composition, microstructure (MEB, XRD), electrochemical performances and corrosion resistance in a 8.7 M KOH solution at 70°C. Single phase alloys were obtained using Y or Cr as additive. Among them, superstoichiometric Cr alloys exhibited improved corrosion resistance during soaking tests. © 2002 Elsevier Science B.V. All rights reserved.

*Keywords:* $AB_5$ type alloys; Cr; Zr; Y; Corrosion resistance

## 1. Introduction

Ni–MH batteries using an $AB_5$ alloy containing Mischmetal (Mm), Ni, Mn, Al and 10 wt.% Co as a negative electrode material are now widely used in portable or electric vehicle (EV) applications. Corrosion resistance of these alloys during cycling is satisfactory to meet the requirements in term of cycle life. Calendar life (i.e., under long periods of rest) must however be improved for EV batteries and other applications like emergency lighting or cordless domestic appliances. Indeed, lifetime is limited by the corrosion of the MH hydrogen-absorbing alloy, generally enhanced by the high temperature (40°C) induced by floating charge. An improvement of corrosion resistance of $AB_5$ alloys during storage is thus aimed at. In addition, market considerations require cheaper alloys with enhanced capacities.

Battery lifetime is limited by alloy corrosion [1–3] which results both from chemical oxidation process by the electrolyte and decrepitation mechanism (fracture of the alloy upon hydriding dehydriding cycles and increase of alloy surface). Since Willems demonstrated the beneficial effect of Co on decrepitation of $AB_5$ alloys [4], many works were being devoted to replace Co by cheaper elements to reduce battery cost while keeping acceptable cycle life. It is now widely accepted that increasing the stoichiometric ratio over 5 reduces alloy decrepitation [5,6] but has no significant effect on its chemical stability [3]. On the other hand, substituting a part of the Mm by Zr [7,8] or adding Y compounds in the negative electrode is beneficial to chemical stability of $AB_5$ alloys [1,9].

In order to improve calendar life of Ni–MH batteries and reduce their cost, the main purpose of this work was to compare the effect on chemical stability in concentrated KOH aqueous solution of the addition of Y, Zr or Cr in low Co content $AB_5$ alloys. Indeed, Cr is well known to reduce corrosion of stainless steel by forming passivation layers.

## 2. Experimental

### 2.1. Preparation and characterisation of alloys

Alloys were elaborated from mischmetal and pure metals, melted in vacuum induction furnace and cooled in conventional conditions (5 cm diameter ingots), rapid cooling (1 cm thickness plates cooled in copper mould with water) or gas atomisation. These alloys were heat-treated for 16 h at temperatures ranged between 900 and 1100°C under vacuum or argon atmosphere. Powders of conventional casted or rapid cooled alloys were obtained by crushing, mechanical grinding and sieving under 75 μm.

---

[*] Corresponding author.

0925-8388/02/$ – see front matter
PII: S0925-8388(01)01671-1

Chemical composition was determined by inductively-coupled plasma (ICP) spectroscopy. Microstructure was examined using scanning electron microscopy (SEM) equipped with an energy dispersive X-ray (EDX) microprobe. In addition, X-ray diffraction (XRD) patterns were measured using a Siemens D5000 diffractometer with Cu K$\alpha$ wavelength.

### 2.2. Measurement of alloy corrosion

The surface behaviour of alloys was characterised by soaking tests. This procedure allows to avoid the pulverisation process (decrepitation) which leads to a continuous increase of the surface in contact with the electrolyte during cycling. A 5-g amount of alloy was immersed in 50 ml of 8.7 M KOH aqueous solution in plastic bottles. In order to avoid possible oxidation by air, the bottles were filled under nitrogen and tightly sealed with PTFE tape. Containers were then continuously shaked in a water heated benchtop incubator at 70°C for 7 days. Since corroded Al is entirely dissolved in the electrolyte, Al content in the solution was analysed by ICP spectrocopy at the end of the etching period. Corrosion rate was then calculated as the ratio between the dissolved amount of Al and the initial amount contained in the 5 g alloy.

During electrochemical cycling, Al eluted from the corroded alloy is entirely trapped in the positive electrode [10]. Al content in the positive electrode, measured by ICP analysis, was thus used as an indicator of alloy corrosion after cycling [3].

### 2.3. Electrochemical evaluation

Alloy powders were mixed with a PTFE binder and 30 wt.% Ni powder INCO 255 (used as an electrical conductor) to manufacture negative electrodes. Five negative limited vented cells per alloy were assembled in plastic cases. They consisted in a single negative electrode isolated by a polyolefine separator from two positive foam electrodes containing $Ni_{1-x-y}Co_xZn_y(OH)_2$ active material and cobalt compounds. The cells were finally filled with a 8.7 M KOH aqueous solution as electrolyte.

Before cycling, cells were charged to 20% state of charge and stored 3 h at 70°C to fasten alloy activation. The complete procedure required another 10 cycles using 16 h charge at C/10 rate (30 mA $g^{-1}$), 1 h rest and a discharge at C/5 rate (60 mA $g^{-1}$) down to 0.9 V cut-off voltage.

Accelerated cycling tests were carried out at C rate (300 mA $g^{-1}$) for 48 min in discharge (80% depth of discharge) and 52 min in charge (8% overcharge). Capacities were periodically measured in the same conditions as for activation. Corrosion rates were measured after cycling.

## 3. Results and discussion

### 3.1. Alloy compositions

Compositions correspond to the general formula $Lm_{0.95}A_{0.05}$ (Ni, Mn, Al, Co)$_{x-0.05}B_{0.05}$ with 5.5 or 7 wt.% Co (Table 1), A=Lm, Zr or Y and B=Ni or Cr. $x$ ranges from 5.15 to 5.20 for balancing the effect of Co content decrease from 10 to 7 or 5.5 wt.% on decrepitation resistance. The mischmetal Lm was La enriched to limit the increase of plateau pressure induced by higher stoichiometric ratio. Most of the alloys are derived from composition 1 (A=Lm, B=Ni) by substituting Cr for B, Zr or Y for A. Other compositions were defined to obtain higher capacities (compositions 2, 10 and 11) and lower cost (compositions 12, 13) by increasing Mn/Al ratio and decreasing Co content.

Table 1
Compositions and ICP analyses of general formula $Lm_{0.95}A_{0.05}$ (Ni, Mn, Al, Co)$_{x-0.05}B_{0.05}$ alloys

| Composition | High Mn/Al ratio | Co content (wt.%) | A/B | $x$ | Alloy | $x$ (ICP) |
|---|---|---|---|---|---|---|
| 1 | No | 7 | Lm/Ni | 5.15 | 1C | 5.20 |
| | | | | | 1R | 5.20 |
| 3 | No | 7 | Lm/Cr | 5.15 | 3C | 5.07 |
| | | | | | 3R | 5.16 |
| | | | | | 3G | 5.10 |
| 4 | No | 7 | Zr/Ni | 5.15 | 4C | 5.19 |
| | | | | | 4R | 5.18 |
| 5 | No | 7 | Y/Ni | 5.15 | 5C | 5.12 |
| | | | | | 5R | 5.13 |
| 2 | Yes | 7 | Lm/Ni | 5.15 | 2C | 5.13 |
| | | | | | 2R | 5.11 |
| | | | | | 2G | 5.17 |
| 10 | Yes | 7 | Zr/Ni | 5.15 | 10R | 5.17 |
| 11 | Yes | 7 | Lm/Cr | 5.20 | 11R | 5.30 |
| 12 | Yes | 5.5 | Zr/Ni | 5.15 | 12R | 5.20 |
| 13 | Yes | 5.5 | Lm/Cr | 5.20 | 13R | 5.16 |

Alloys labelled by composition number and cooling process (C: conventional casting, R: rapid cooling or G: gas atomisation).

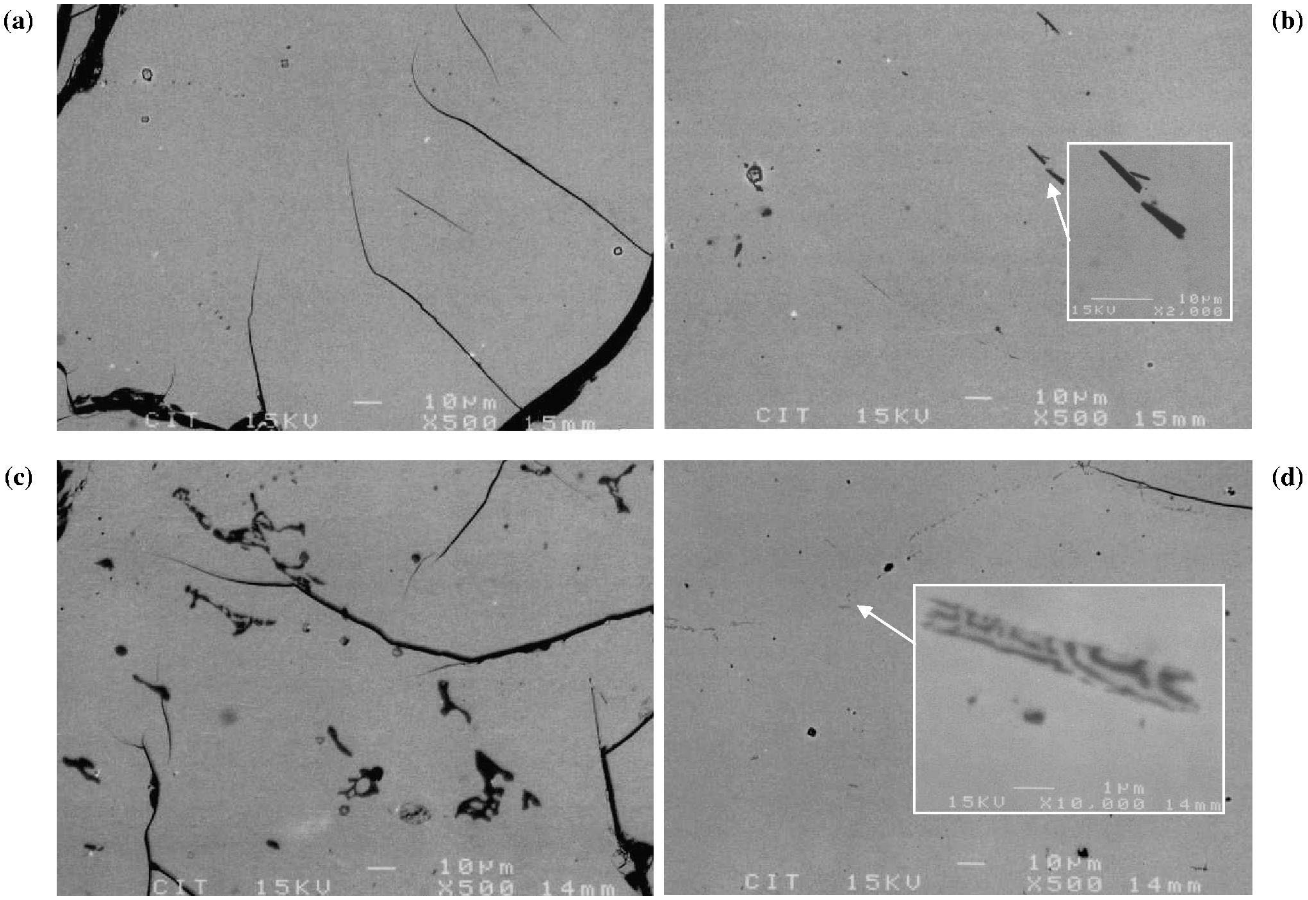

Fig. 1. SEM observations of conventionally cast alloys 2C (a), 3C (b), 4C (c) and 5C (d).

In Table 1, elaborated alloys are labelled by their composition number followed by a letter which indicate the cooling process (C: conventional casting, R: rapid cooling and G: gas atomisation). Stoichiometric ratios *x*, measured by ICP analyses, are scattered between 5.07 and 5.30 due to the addition of experimental errors from each compound content determination.

### 3.2. Conventionally cast alloys

On the whole, conventionally cast alloys exhibit (SEM) second phases. Rare earth enriched (bright areas) or rare earth oxide (polygonal dark grey areas) precipitate in the matrix of alloys 1C and 2C (Fig. 1a). Few areas looking like eutectic are detected in alloy 5C (Fig. 1d). Global EDX microanalysis shows they are enriched in transition metal and Al. Cr flakes precipitated in alloy 3C (Fig. 1b). 2 to 3% of $ZrNi_5$ type second phase precipitated in alloy 4C (Fig. 1c), as determined by EDX microanalysis and confirmed by XRD patterns.

After 7 days soaking in 8.7 M KOH at 70°C, the conventional cast alloys 1C to 5C exhibit similar corrosion rates ranged between 2.1 and 2.2% (Table 2).

Cycling test results (Table 2 and Fig. 2) show that alloy 4C with Zr additive exhibits a lower capacity than alloy 1C. This was probably due to the precipitation of the $ZrNi_5$ type phase which reduces the amount of $CaCu_5$ type matrix but should not change significantly its stoichio-

Table 2
Electrochemical and soaking tests evaluation of conventional cast alloys

| Alloy | High Mn/Al ratio | Co content (wt.%) | A/B | Corrosion rate after soaking test (%) | Capacity (mAh $g^{-1}$) | Corrosion rate after 300 cycles (%) |
|---|---|---|---|---|---|---|
| 1C | No | 7 | Lm/Ni | 2.2 | 290 | 5.0 |
| 3C | No | 7 | Lm/Cr | 2.2 | 301 | 5.0 |
| 4C | No | 7 | Zr/Ni | 2.1 | 281 | 4.9 |
| 5C | No | 7 | Y/Ni | 2.1 | 298 | 6.2 |
| 2C | Yes | 7 | Lm/Ni | 2.1 | 322 | 11.2 |

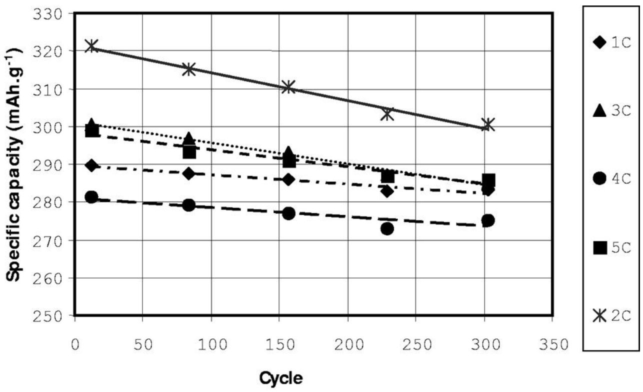

Fig. 2. Cycling test results of alloys elaborated by conventional casting.

metric ratio. On the contrary, the capacities of alloys 3C and 5C with Cr and Y additive are 10 mAh g$^{-1}$ higher than for alloy 1C. This could be the result of a lower matrix stoichiometric ratio partly due to the precipitation of B element enriched phases. As expected, alloy 2C capacity reaches more than 320 mAh g$^{-1}$, which can be attributed to the increase of the Mn/Al ratio. Corrosion rates after 300 cycles (Table 2) are almost the same (around 5%) in the case of alloys without additive (1C) and with Cr or Zr additive (3C and 4C). But a corrosion higher by 1.2% is measured using Y as additive (alloy 5C) and a sharp corrosion increase to 11.2% is observed for the high capacity alloy 2C.

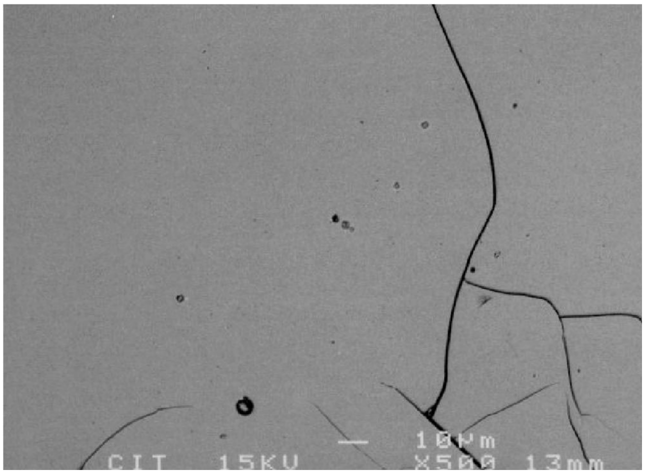

Fig. 3. SEM observations of rapid cooled alloy 3R.

### 3.3. Rapid cooled alloys

When cooling rate is increased, a metallurgic improvement is noticed for alloys 1R, 2R, 5R and particularly 3R (Fig. 3) according to SEM examinations and XRD. The latter four alloys appear nearly single phase, but rapid cooling treatment does not allow Zr element to enter inside alloy matrix: 2 to 3% of precipitates are still observable in alloy 4R.

Soaking test corrosion rates (Table 3) are reduced to 1.9% for alloy 3R with Cr additive as for alloys 4R and 5R with Zr (1.9%) and Y (1.8%) additives. On the other hand, corrosion rate of alloys 1R and 2R without additive are increased to 2.4%, whatever the Mn/Al ratio. It thus appears that rapid cooling enhances the chemical stability of alloys containing Cr, Zr or Y but is detrimental for alloys without additives.

Regarding electrochemical evaluation (Table 3), no significant change of initial capacity between rapid cooled and conventionally cast alloys of the same nominal composition is observed.

Corrosion rates of rapid cooled alloys after 300 cycles are always lower than conventional cast ones. This effect is generally more pronounced in the case of compositions 1 and 2 without additive (corrosion rate decreased by more than 35%) than for compositions with additives (about 30% reduction). This corrosion rate reduction can be explained by the chemical stability improvement in the case of alloys with additives. Regarding the other cases (compositions 1 and 2), chemical stability is found to slightly decrease when using rapid cooling. Therefore, the improvement of their corrosion resistance during cycling should be due to an enhanced decrepitation resistance when alloys are rapid cooled. Finally, it should be noticed that corrosion rate during cycling of alloys with Y additive, elaborated either by conventional casting or by rapid cooling, is higher than that of alloys with Cr and Zr

Table 3
Electrochemical and soaking tests evaluation of rapid cooled alloys

| Alloy | High Mn/Al ratio | Co content (wt.%) | A/B | Corrosion rate after soaking test (%) | Capacity (mAh g$^{-1}$) | Corrosion rate after 300 cycles (%) |
|---|---|---|---|---|---|---|
| 1R | No | 7 | Lm/Ni | 2.4 | 286 | 1.2 |
| 3R | No | 7 | Lm/Cr | 1.9 | 299 | 3.5 |
| 4R | No | 7 | Zr/Ni | 1.9 | 280 | 2.2 |
| 5R | No | 7 | Y/Ni | 1.8 | 298 | 4.1 |
| 2R | Yes | 7 | Lm/Ni | 2.4 | 324 | 7.2 |
| 10R | Yes | 7 | Zr/Ni | 1.9 | 304 | 10.1 |
| 11R | Yes | 7 | Lm/Cr | 1.3 | 318 | 6.2 |
| 12R | Yes | 5.5 | Zr/Ni | 2.0 | 303 | 10.6 |
| 13R | Yes | 5.5 | Lm/Cr | 1.5 | 317 | 6.7 |

Table 4
Electrochemical and soaking tests evaluation of gas atomised alloys

| Alloy | High Mn/Al ratio | Co content (wt.%) | A/B | Corrosion rate after soaking test (%) | Capacity (mAh $g^{-1}$) | Corrosion rate after 300 cycles (%) |
|---|---|---|---|---|---|---|
| 2G | Yes | 7 | Lm/Ni | 1.9 | 321 | 8.6 |
| 3G | No | 7 | Lm/Cr | 1.2 | 308 | 7.4 |

additives. As the alloy 5R exhibits a better chemical stability than alloys 3R and 4R, it seems that Y is rather detrimental to decrepitation resistance.

Following these results and in order to combine a high chemical stability, a high capacity, an acceptable resistance against corrosion during cycling and low cost, alloys with low Co content (7 and 5.5 wt.%), high Mn/Al ratio and Zr or Cr additives were elaborated by rapid cooling. Alloys 11R and 13R with Cr consist in a single $CaCu_5$ type phase as determined from SEM examinations and XRD measurements, but $ZrNi_5$ type precipitates are still observed in Zr alloys 10R and 12R. The results of soaking tests and electrochemical evaluation are reported in Table 3.

Compared to alloy 2R, Zr addition (either with 7 or 5.5 wt.% Co) induces a reduction of the corrosion rate after soaking by more than 16% but at the expense of a capacity decrease by 20 mAh $g^{-1}$. In addition corrosion rates during cycling are increased by more than 40%. On the other hand, alloys 11R and 13R with Cr additive exhibit not only an enhanced chemical stability (less than 1.5% corrosion after soaking test), but also a corrosion reduction by more than 7% after cycling and only a slight capacity decrease by 5 mAh $g^{-1}$, compared to alloy 2R. These results are likely to be due to Cr addition. Indeed, alloy 13R with 5% Co exhibits a higher corrosion resistance than alloy 2R with 7 wt.% Co and without Cr.

### *3.4. Gas atomised alloys*

As in the case of rapid cooling, a metallurgic improvement is noticed for alloys 2G and 3G which appears nearly single phase. According to SEM examinations and XRD, almost all Cr enters the matrix when atomising alloy 3G.

Compared to conventional casting, gas atomisation improves corrosion resistance of both alloys during soaking test (Table 4). Regarding Cr alloy (composition 3), it is consistent with the result observed previously: increasing cooling rate increases chemical stability of alloys with Cr additive. The opposite effect is however observed when comparing alloy 2C to 2R. The higher chemical stability of alloy 2G compared to alloy 2R could be explained as follow: rapid solidification processes induce composition heterogeneity between the surface and the bulk of cast pieces. In the case of rapid cooled alloys, heat treatment cannot completely homogenise the alloy because the ingot breaks during cooling, contrary to gas atomised particles. Composition heterogeneity are likely to depend on the considered component.

Electrochemical evaluation (Table 4) shows a similar value of capacity for each tested composition, whatever the cooling rate, particularly in the case of composition 2. It confirms that cooling rate has no impact on initial capacity of alloys. On the other hand, increasing cooling rate sharply increases alloy stability during cycling. Indeed, alloy 3G with Cr shows a corrosion after 300 cycles 14% less than alloy 2G. Cr addition combined with rapid cooling processes seems thus beneficial to chemical and cycling stability, without inducing too high capacity losses.

## 4. Conclusions

Alloys of general formula $Lm_{0.95}A_{0.05}$ (Ni, Mn, Al, Co)$_{x-0.05}B_{0.05}$ containing 5.5 or 7 wt.% Co with A=Lm, Zr or Y and B=Ni or Cr were elaborated using different cooling rates. They were characterised in terms of chemical composition, microstructure, chemical stability during storage in 8.7 M KOH solution at 70°C for 7 days, electrochemical capacity and corrosion rate during cycling.

The main results are:

- Increasing cooling rate is beneficial to chemical stability when considering Zr, Cr or Y doped alloys.
- Cr precipitates observed in the conventionally cast alloy with M=Cr can be dissolved in the $CaCu_5$ type matrix using rapid cooling techniques, but $ZrNi_5$ type precipitates were always observed when M=Zr whatever the cooling rate.
- Y addition seems to be detrimental to decrepitation resistance and Zr addition to alloy capacity.
- Alloys with high Mn/Al ratio and Cr additives elaborated using high cooling rates allow to achieve both high electrochemical capacity and enhanced chemical stability. Their corrosion resistance during cycling is still to be improved however.

## Acknowledgements

The European Commission in the framework of the BRITE EURAM III program (contract CT98-0734) funded this research.

## References

[1] H. Kaïa, T. Ookawa, J. Alloys Comp. 231 (1995) 598.

[2] M. Kanda, M. Yamamoto, K. Konno, Y. Satoh, M. Hayashida, M. Suzuki, J. Less-Common Metals 172–174 (1991) 1227.

[3] P. Leblanc, C. Jordy, B. Knosp, Ph. Blanchard, J. Electrochem. Soc. 143 (3) (1998) 860.

[4] J.J.G. Willems, Philips J. Res. 39 (Suppl. 1) (1984).

[5] P.H.L. Notten, R.E.F. Einerhand, J.L.C. Daams, J. Alloys Comp. 310 (1994) 221.

[6] J.M. Cocciantelli, P. Leblanc, G. Caillon, B. Knosp, Ph. Blanchard, J. Atkin, J. New Mater Electrochem. Syst. 2 (1999) 151.

[7] T. Sakai, M. Miyamura, M. Kuriyama, A. Kato, K. Oguro, H. Ishikawa, J. Electrochem. Soc. 137 (3) (1990) 795.

[8] Hazama, Tokuichi, Eur. Pat. EP 0 451 575 A1, 1991.

[9] K. Furukawa, T. Tanaka, Y. Matsumara, M. Wataba, M. Oshitani, Yuasa-Jiho 82 (1997) 27.

[10] J.M. Cocciantelli, P. Bernard, S. Fernandez, J. Atkin, J. Alloys Comp. 253–254 (1997) 642.